Anthropogenic carbon dioxide in the South Atlantic western basin

Aida F. Ríos[1*], Marcos Vázquez-Rodríguez[1], X. A. Padin[1], Fiz F. Pérez[1]

[1] Instituto de Investigaciones Marinas, CSIC, Eduardo Cabello 6, E-36208 Vigo, Spain

*Corresponding author. Email: aida@iim.csic.es. Tel.: +34 986 231930 Ext. 371. Fax: +34 986 292762

Abstract

The meridional WOCE line A17 was conducted during the austral summer of 1994 parallel to the eastern South American coast, from 55°S to 10°S, where one of the main limbs of the North Atlantic Deep Water (NADW), i.e., the southward-flowing Deep Western Boundary Current (DWBC) is found. Full–depth profiles of pH, total alkalinity and total inorganic carbon were measured and checked with analytical CO_2 certified reference materials (CRMs), providing a high-quality dataset with good internal consistency for the CO_2 system parameters that is well suited for anthropogenic CO_2 (C_{ANT}) estimation. For the first time in the western Atlantic basin the C_{ANT} has been calculated using four independent approaches and results are compared. The methods considered are the CFC-based TTD method and the φC_T^o, TrOCA and ΔC^* carbon-system-based back-calculation methods. All four methods have produced C_{ANT} distribution patterns that are in general good agreement: maximum concentrations of C_{ANT} (50-60 µmol kg^{-1}) are predicted for the upper warm South Atlantic central waters from the tropical gyres, while the minima (~5 µmol kg^{-1}) are located in the old northward-flowing branch of Circumpolar Deep Water. There are, however, some discrepancies detected. The TrOCA method yields the highest overall [C_{ANT}] values, even over the theoretical limit of C_{ANT} saturation for 1994 in the upper layers. The ΔC^* approach consistently yielded negative estimates of C_{ANT} below 2800 dbar, even after correcting a reported -8 µmol kg^{-1} bias in the alkalinity measurements of the WOCE A17 line. The main overall difference between the four methods corresponds to the relative C_{ANT} maximum associated with the lower limb of NADW: this structure is well identified in the φC_T^o and TTD methods but seems to disappear in the case of TrOCA and ΔC^*. In agreement with other intercomparison studies of C_{ANT}, the specific inventories are significantly higher (~45%) than those reported in the GLODAP database obtained from the ΔC^* method. This suggests that the South Atlantic stores more C_{ANT} than initially expected, particularly towards the southernmost tip of the WOCE A17 line, close to the Southern Ocean. The φC_T^o, TrOCA and TTD methods confirm an increasing tendency of C_{ANT} specific inventories south from the Equator, while the ΔC^* method shows a decreasing trend south from 35ºS.

1. Introduction

The ocean plays a major role in the global carbon cycle by sequestrating annually 2.2 ±0.4 Pg C out of the total 8.0 ±0.5 Pg yr^{-1} of anthropogenic CO_2 (C_{ANT}) emitted to the atmosphere as a result of activities such as fossil fuel burning, land use changes, deforestation and cement production (Canadell et al., 2007). The Atlantic Ocean alone contributes with a share of 38% to the anthropogenic oceanic carbon storage, even though it only represents 29% of the global ocean surface area (Sabine et al., 2004). The formation of deep waters in the North Atlantic (NADW) and Southern Ocean (Antarctic Bottom Water; AABW) enhances significantly the Atlantic storage of C_{ANT} (Lo Monaco et al., 2005). An important branch of the NADW, the Deep Western Boundary Current (DWBC), flows southwards from the Irminger and Labrador Seas and communicates with the South Atlantic basin through the Equatorial channel (Steinfeldt et al. 2007). The DWBC splits into eddies at 8ºS such that, southwards from this latitude, the NADW is carried into the South Atlantic Ocean by migrating eddies, rather than by a continuous flow (Dengler et al., 2004). The eastward deflection of the southward-flowing DWBC has also been observed in the NADW domain (Weiss et al., 1985; Richardson and Schmitz, 1994; Rhein et al., 1995; Andrié, 1996; Mercier and Arhan, 1997; Arhan et al., 1998) along and just south of the Equator. On the other hand, model-based studies have suggested that a weakening in the thermohaline circulation and increases of sea surface temperature can potentially reduce ocean carbon uptake by up to 50% and that such reductions are only partly counterbalanced by changes in the marine biological cycle (Sarmiento and Le Quére, 1996; Sarmiento et al., 1998).

The Atlantic sector of the Southern Ocean withholds moderate concentrations of C_{ANT} yet its massive volume turns it into one of the largest carbon reservoirs of this basin (Vázquez-Rodríguez et al., 2009b). Manabe and Stouffer (1993) spotted from model results a potential modification of the ocean carbon sink in a vast region of the Southern Ocean, where increased rainfall would lead to surface freshening and increased stratification. The increased stratification

62 reduces the downward flux of carbon and hinders the air-sea heat exchanges causing an overall
63 decrease of the oceanic C_{ANT} uptake in the Southern Ocean (Sarmiento et al. 1998). Recent
64 estimates of CO_2 sink in the Southern Ocean showed a weakening between 1981 and 2004
65 which was attributed to the observed increase in Southern Ocean winds resulting from human
66 activities (Le Quére et al., 2007). The response of the carbon sink in the Southern Ocean to the
67 changes in the wind stress is currently under debate (Böning et al., 2008). Most of the above-
68 mentioned results were obtained from model-based studies and, given the importance of the
69 Southern Ocean in the context of global ocean carbon sink, the acquisition and analysis of high-
70 quality field data remain essential tasks to obtain the best possible C_{ANT} estimates.
71
72 Over the years, a series of methods have been developed to retrieve the relatively small
73 (3%) C_{ANT} signal from the large total inorganic carbon (C_T) pool in the oceans. One of the issues
74 concerning C_{ANT} is that it cannot be measured directly. Consequently, the so-called back-
75 calculation techniques were developed to estimate C_{ANT} indirectly from direct observation of
76 other tracers. This technique was first applied in the pioneering works of Brewer (1978) and
77 Chen and Millero (1979). The methodology basis consists in separating from the measured C_T
78 the individual contributions or background signals from Organic Matter Remineralization
79 (OMR) and dissolution of calcium carbonate species that had occurred since the water mass
80 formed (it was last in contact with the atmosphere). Following the earlier concept of preformed
81 nutrient defined by Redfield et al. (1963), the preformed total inorganic carbon (C_T^o) was
82 analogously defined (C_T of the water mass right after formation). This term and the air-sea CO_2
83 disequilibrium (ΔC_{dis}) are also subtracted from the measured C_T. The C_T^o term has not remained
84 constant after the pre-industrial era. The water masses have gradually formed in contact with a
85 continuously altered atmosphere by human activity. Therefore, the C_T^o term tracks the imprint
86 of C_{ANT}, which can be retrieved by subtracting a "zero-C_{ANT}" reference from this preformed
87 property.
88

Lo Monaco et al. (2005) reevaluated the specific inventories of C_{ANT} for the Southern Ocean using an observational carbon-dependent back-calculation technique based on the one from Körtzinger et al. (1998) that had been applied in the North Atlantic. They found higher values (52-70 mol C m^{-2}) than those computed from the ΔC* method (Gruber et al., 1996) (29-46 mol/m^2) at latitudes between 30-47ºS in the Atlantic. Recently, a series of different C_{ANT} methods like the TTD, TrOCA and $\varphi C_T°$ approaches (Waugh et al., 2006; Touratier et al., 2007; Vázquez-Rodríguez et al., 2009a) have confirmed Lo Monaco et al.'s (2005) findings and corroborate that C_{ANT} inventories in the Southern Ocean could be, in fact, much larger than previously estimated (Vázquez-Rodríguez et al., 2009b).

The present work uses data from the WOCE A17 cruise, which runs parallel to the eastern South American coast, to obtain the C_{ANT} distribution and inventories by applying a recent observational carbon-based approach, the $\varphi C_T°$ method (Vázquez-Rodríguez et al., 2009a) and the TrOCA method (Touratier et al., 2007). The obtained results are then compared with C_{ANT} estimates from other back-calculation techniques, namely: the ΔC* (Gruber et al., 1996) and the CFC–based TTD approach (Waugh et al., 2006). This practice was never performed before in the western Atlantic basin.

2. Dataset and methodology

The measurements used in this work were performed onboard the R/V *Maurice Ewing* from January 4th until March 21st 1994 during the CITHER-2 / WOCE A17 cruise, framed within the WOCE/French Project CITHER (CIrculation THERmohaline). This quasi-meridional section was complemented by three short transverse lines to the continental slope at nominal latitudes 35°S, 13°S, and 10°N (Fig. 1a). These transversal legs are not considered for the estimation of C_{ANT} in the present study. The water samples were collected at 32 depth levels, from the surface down to 15 m above the bottom. The average horizontal spatial resolution of 30 nautical miles between stations was increased near the Equator and prior to stations that

displayed steep bathymetric profiles. A general presentation of the cruise, and a thorough description of the data used in this paper is provided in Groupe CITHER-2 (1995, 1996). Also, the quality-controlled database is publicly available (http://cdiac.ornl.gov/oceans/woce_a17c.html) as well as the PI recommend corrections (section 3.7 at http://cdiac.ornl.gov/oceans/ndp_084/ndp084.html).

The pH measurements were originally reported in the NBS scale, as described in Pérez and Fraga (1987a). Total alkalinity (A_T) measurements were performed every three stations using a single end point titration technique (Pérez and Fraga, 1987b; Mintrop et al., 2002). Total inorganic carbon (C_T) was directly measured onboard with a coulometric method using a "Single Operator Multi–Parameter Metabolic Analyzer (SOMMA)" (Johnson et al., 1993). Where not measured, C_T was calculated additionally from A_T and pH_{NBS} measurements using the thermodynamic equations of the carbon system and the CO_2 dissociation constants from Dickson and Millero (1987; refit from Mehrbach et al. 1973). The measured and calculated C_T values agreed within ±1.6 μmol kg^{-1} (Ríos et al., 2005). Additional physical-chemical properties used in the present work such as salinity, temperature, dissolved oxygen, nutrients and CFC-11 were measured using standard methodologies, which are detailed in the cited data reports. The accuracy of the measured CO_2 parameters was evaluated using "Certified Reference Materials" (CRMs) supplied by Dr. A.G. Dickson (Univ. of California). The CRM samples were analyzed routinely for a total of 163 C_T measurements during the cruise, with an average difference from the certified C_T value (2115.15 μmol kg^{-1}) of ±1.6 μmol kg^{-1}. The average of 146 CRM analyses for A_T was also in good agreement with the certified value to ±1.7 μmol kg^{-1} (Ríos et al., 2005). An offset in the A_T data of -8 μmol kg^{-1} (i.e., -0.32%) was later detected for the WOCE A17 line and reported by Ríos et al. (2005). The nutrients were determined by segmented flow analysis with a Technicon II Autoanalyzer (Mouriño and Fraga,1985; Alvarez-Salgado et al.,1992). The accuracy of nitrate and phosphate was ±0.1 and ±0.01 μmol kg^{-1}, respectively.

146 Regarding C_{ANT} estimation, four methods have been considered in this study: the TTD
147 (Waugh et al., 2006), ΔC* (Gruber et al., 1996), TrOCA (Touratier et al., 2007) and φC_T^o
148 (Vázquez-Rodríguez et al., 2009a,b). The ΔC* method was previously applied to the GLODAP
149 dataset and results were accessed from the GLODAP website
150 (http://cdiac.ornl.gov/oceans/glodap/Glodap_home.htm), as well as the CFC12-age data. The
151 results of the C_{ANT} estimates from the TTD method were downloaded from the following
152 website: https://jshare.johnshopkins.edu/dwaugh1/public_html/Cant/. On the basis of the
153 variables needed to compute C_{ANT}, the methods here mentioned can be classified into two
154 groups: a) the carbon-based methods (ΔC*, TrOCA and φC_T^o), which typically require
155 measurements of C_T, A_T, oxygen, temperature, salinity and eventually some nutrient analysis.
156 The reported A_T offset of -8 μmol kg^{-1} has been considered when calculating C_{ANT} from back-
157 calculation methodologies. In the case of the GLODAP-ΔC* results, the -8 μmol kg^{-1} A_T offset
158 translates directly into a 4 μmol kg^{-1} C_{ANT} offset (according to the formulation in Gruber et al.,
159 1996), which has been added to the original GLODAP estimates of C_{ANT}; b) the Transient-
160 Tracer-based methods (TTD) that commonly use CFC-11 or CFC-12 concentration
161 measurements as proxies of the anthropogenic CO_2 signal. The uncertainties in C_{ANT} estimates
162 for the ΔC*, TrOCA, φC_T^o, and TTD methods are ±7.9, ±6.2, ±5.2, and ±5.0, μmol kg^{-1},
163 respectively. A summary of the C_{ANT} methods used in this work can be found in Vázquez-
164 Rodríguez et al. (2009b).
165
166 The amount of dissolved $CaCO_3$ (ΔCa) in the water column is one of the fundamental terms
167 in C_{ANT} back-calculation methodologies. The ΔCa is defined as $\Delta Ca = ½ (PA_T - PA_T^o)$ in terms
168 of the measured A_T and preformed A_T (A_T^o), i.e., the alkalinity of the considered water mass at
169 the moment of formation, when it was last in contact with the atmosphere. The potential
170 alkalinity term (PA_T) is defined as $PA_T = A_T + NO_3 + PO_4$ (Robertson et al., 1994). The OMR
171 does not affect the PA_T in the water column but carbonate shifts caused by $CaCO_3$ dissolution
172 still increase PA_T by a factor of two. (Vázquez-Rodríguez et al., 2009a). A plot showing the

vertical distribution of ΔCa along the WOCE A17 line is shown in Fig. 2. The corresponding PA_T^o term in the ΔCa expression was calculated as in Vázquez-Rodríguez et al. (2009a).

3. Results

The main water masses found on the WOCE A17 section are clearly identified from the temperature, salinity and silicate distributions (Figure 2). The warm and saline South Atlantic Central Water (SACW) is predominantly present above 1000 dbar along the whole section. There exist several varieties of this water mass that are well described in Mémery et al. (2000) (hereinafter M'00). The Antarctic Intermediate Water (AAIW) is characterised by its salinity minimum (34.1-34.5) that extends from the Subantarctic Front (46ºS) northwards, between 800 and 1000 dbar. Under the AAIW at ~1000 dbar and south from 20ºS there is a relative maximum of temperature (3.2 ºC) and silicate (45 μmol kg^{-1}) corresponding to the upper Circumpolar Deep Water (*u*CDW). The North Atlantic Deep Water (NADW) extends southwards along the section, characterised by an ample salinity maximum (>34.9) located between 1000 and 3500 dbar. Several varieties of NADW have also been thoroughly described in M'00, most importantly its upper and lower limbs (*u*NADW and *l*NADW, respectively) that are identified in Fig. 2. In the Equatorial region at about 1800 dbar there is a relative salinity maximum (~34.95) associated to a minimum silicate signal (~20 μmol kg^{-1}) that identifies the *u*NADW branch. The *l*NADW limb is located immediately below (~3500 dbar), with slightly lower salinity and higher silicate values (~34.90 and 35 μmol kg^{-1}, respectively) than the upper branch. The maximum silicate values recorded are located at the southern end of the section. They are associated to the lower limb of the CDW (*l*CDW; $[SiO_2]\approx120$ μmol kg^{-1}) and to the Antarctic Bottom Water (AABW) ($[SiO_2]$ >125 μmol kg^{-1} and θ <0 ºC) (M'00).

The biological component (AOU/R_C) in the general back-calculation equation represents a measure of the OMR contribution to the measured C_T signal. This term reaches values of up to

85 μmol kg^{-1} in the case of AABW and has two relative minima (~49 μmol kg^{-1}, when using the R_C=1.45 proposed by Anderson and Sarmiento, 1994) associated to the upper and lower NADW limbs that evolve into a single relative AOU minima south from 20ºS (Fig. 2; M'00). The absolute AOU maximum is located at the core of the SACW, between 500 and 700 dbar north from 15ºS. This layer of the ocean accumulates high loads of organic matter from the Equatorial upwelling regions, and the AOU/R_C term can amount up to 120 μmol kg^{-1} of C_T. The lowest AOU values in the section correspond to young recently ventilated surface waters (lowest observed CFC12 age) around 40ºS (M'00). Similarly, both limbs of NADW are characterised by their relative CFC12 age minima of ~40 yr. However, it must be noted that using CFC12 concentrations to infer water mass ages tends to underestimate ages in waters older than 25 years (Matear et al., 2003). In spite of the methodological biases, the waters found in the band between 40ºS and the Equator and below 2000 db are indeed very old water masses.

As introduced earlier, the dissolution of $CaCO_3$ (ΔCa) also affects the C_T content of a water parcel. The ΔCa is largest in the AABW and bottom waters in general throughout the section, where the oldest water masses are found (Chung et al., 2003). Although there is a general trend of ΔCa to increase with depth, an evident relative minimum of ΔCa (12 μmol kg^{-1}) is observed associated to the moderately young *u*NADW. These values are in contrast with the relative ΔCa maximum from the little-ventilated SACW/AAIW between 600 and 800 dbar, placed immediately above the *u*NADW. Alternatively, the fairly good correlation between the observed ΔCa and silicate fields indicates that most dissolved $CaCO_3$ is advected from Antarctic waters (namely, AABW and CDW). This relationship is well documented in the literature (Broecker and Peng, 1982; Ríos et al., 1995; Pérez et al., 2002) and draws a clear line of demarcation between waters with strong Antarctic influence and the rest. The high correlation stems from the relationship between the dissolution of opal and calcium carbonate.

225 Independently of the C_{ANT} reconstruction method used, the maximum values of C_{ANT} (50-
226 60 μmol kg^{-1}, i.e., around the corresponding C^{sat}_{ANT} for 1994) are always found in the warm
227 upper waters from the subtropical gyres (Fig. 3). In the C_{ANT} distribution obtained with the φC_T^o
228 method the minimum values (~5 μmol kg^{-1}) are located at the oldest water masses (CFC12 age
229 ~50 yr) near the 3500 dbar level between the *u*NADW and *l*NADW, where the influence of
230 *l*CDW is slightly more noticeable (M'00). Asides from this, there exists a relative minimum of
231 C_{ANT} at 1000 dbar north of 15ºS. It coincides with the penetration northwards of *u*CDW (M'00),
232 which erodes the relative maxima of the slightly more ventilated, younger, southward-flowing
233 *u*NADW and *l*NADW. South from 30ºS, the high burdens of C_{ANT} in subsurface waters reach
234 down to 1200 dbar, while bottom waters show C_{ANT} concentrations of approximately 10 μmol
235 kg^{-1}. In the deepest end of the section, south of 40ºS, there is a slight increase of C_{ANT} with
236 respect to the surrounding waters that is likely caused by the penetration northwards of the
237 AABW.

238

239 The C_{ANT} estimates from the TTD approach do not depend on the measurements of
240 carbon system parameters yet its results are in remarkable resemblance with the ones from the
241 φC_T^o, most notably: the C_{ANT} distributions at the subsurface, at the *u*NADW and *l*NADW
242 associated maxima north of 15ºS, and the relative minima from the spreading of *u*CDW, *l*CDW
243 and the deep AABW. There are, however, discrepancies between the TTD and φC_T^o results.
244 Amongst the most relevant discrepancies there is the larger penetration of the high-C_{ANT} from
245 the uppermost layers waters down to ~1200 dbar uppermost layers south from 30ºS predicted by
246 the TTD, compared with the φC_T^o method. On the contrary, under 2000 dbar the φC_T^o estimates
247 are higher on average (3±2 μmol kg^{-1}) than the TTD ones, except in the case of the *l*NADW
248 where the TTD approach has produced the highest C_{ANT} estimates.

249

The C_{ANT} fields produced by the ΔC* method included in the GLODAP database (Key et al., 2004) were corrected by the A_T offset (Ríos et al.,2005). Although this correction removes 23% of the negative values of C_{ANT}, the ΔC* method keeps showing negative C_{ANT} concentrations below the 2800 dbar level in the WOCE A17 section (Fig. 3). These negative C_{ANT} estimates were not considered for inventory calculations. Above this depth level the estimates are relatively similar to those from the φC_T^o method, reproducing the relative maximum associated to the *u*NADW north of 15ºS and the relative minimum of the *u*CDW. However, south from 30ºS the layers with the largest concentrations of C_{ANT} are thicker (by ~250 meters, likely due to the AAIW influence) than those predicted by the φC_T^o method (Fig. 3).

The TrOCA approach has the convenience of being a very straightforward C_{ANT} method to apply, since it is based on one simple equation that can be applied to the global ocean. The obtained C_{ANT} fields through this method follow the same general trends described above for the rest of methods. It reproduces well the *u*CDW relative minimum north of 15ºS and the moderate C_{ANT} values from the AABW. The thickness of the high-C_{ANT} upper layers is similar to that from the TTD and reaches deeper than in the case of the φC_T^o and ΔC* methods. Nonetheless, the TrOCA method has generally yielded the highest C_{ANT} estimates. The absolute maximum C_{ANT} values in the upper SACW are the highest of all four methods, reaching even over the theoretical upper-limit of C_{ANT}^{sat} for 1994 (C_{ANT}^{sat} is the theoretical saturation concentration of C_{ANT} for surface waters in equilibrium with the atmospheric CO_2 levels when the cruise was conducted). The main differences with the other methodologies are found in the slightly higher values associated to the relative minimum of the *l*CDW and in the lower values (~5 μmol kg^{-1}) spreading between 3000 and 4000 dbar all along the section, especially with respect to the φC_T^o and TTD methods. In addition, the relative maximum of the *l*NADW predicted by the latter two methods disappears in the case of TrOCA, while the C_{ANT} estimates for the AABW fall halfway

in the range between the φC_T^o and TTD results. Finally, the relative maximum in the *u*NADW is also the highest of all four methods.

4. Discussion

One of the main goals in C_{ANT} estimation is to be able to come up with an educated guess of how much of it is stored in the ocean. Since C_{ANT} cannot be measured directly and there is no absolute reference against which results can be checked unequivocally, a comparison of the latitudinal variability (according to different estimation methodologies) of the specific C_{ANT} inventories is well justified (Fig. 4).

The vertically integrated C_{ANT} fields from the φC_T^o and TrOCA methods are found to be in outstanding agreement, always within the uncertainties of either method. It is remarkable to see such a concurrence given the different C_{ANT} vertical gradients described by the two methods (Fig. 3). The observed differences stem mainly from the particular zero-C_{ANT} references in each approach. The similarities between the φC_T^o and TrOCA specific inventories of C_{ANT} likely comes from a compensation of C_{ANT} between the uppermost and deeper layers: while the φC_T^o method predicts lower C_{ANT} concentrations in the upper layers than TrOCA, the opposite occurs in deeper layers. When vertically integrated in the water column, the concentration values get, therefore, compensated. The lower surface concentrations in the φC_T^o approach derive from considering the temporal variability of the air-sea CO_2 disequilibrium ($\Delta\Delta C_{dis}$), compared to the TrOCA approach. On the other hand, the slightly higher bottom estimates of the φC_T^o method are the outcome of the A_T^o parameterization that was obtained taking subsurface layer observations as a reference of water mass formation conditions.

The C_{ANT} intercomparison work from Vázquez-Rodríguez et al. (2009b) included an analogous comparison for the φC_T^o and TrOCA methods (amongst others) in the WOCE A14, which runs parallel to the west African coast along 10ºW covering a similar latitudinal range to the WOCE A17. In that work, the specific inventories of C_{ANT} calculated from the φC_T^o are higher than the ones from the TrOCA method south from 20ºS, unlike in the WOCE A17, where results are more alike. This discrepancy likely stems from the fact that, unlike in the present study, the TrOCA method showed large volumes of C_{ANT}-depleted waters in the deep South Atlantic region (south from 20ºS) of the WOCE A14 section. A recent publication (Yool et al., 2010) based on a comparison of C_{ANT} estimates from the TrOCA method with model outputs questions the theoretical foundations of the TrOCA approach and reveals very large biases (up to 50%) at regional level, suggesting that a satisfactory universal TrOCA parameterisation is not achievable.

The φC_T^o and TrOCA methods give specific inventories of C_{ANT} over the TTD ones, most notoriously in the latitudinal band between the Equator and 25ºS. This seems to be the direct result of the lower C_{ANT} values predicted in this region by the TTD between 1000 and 2000 dbar (Fig. 3), compared with the TrOCA and φC_T^o methods. Contrastingly, the opposite occurs with the high TTD values for the *l*NADW. In spite of these discrepancies, the results obtained for the WOCE A14 in Vázquez-Rodríguez et al. (2009b) for the eastern Atlantic basin showed very similar specific inventories of C_{ANT} for the TTD and φC_T^o methods. This is likely due to the fact that the deep waters in the eastern basin are older than those in the western one, and have therefore smaller amounts of C_{ANT} and CFCs (Vázquez-Rodríguez et al., 2009b) that would yield lower methodological discrepancies. Regarding the difference of results here obtained for the WOCE A17 line, they are likely caused by the fact that the TTD approach assumes a globally constant mixing (Δ) to advection (Γ) ratio $\Delta/\Gamma=1$ that might not be particularly representative of the ocean dynamics in the North Atlantic given the strong influence of the Meridional Overturning Circulation. Actually, it is most probable that the two NADW branches

would not share the same Δ/Γ ratio since advection is likely to gain relevance over mixing in the upper NADW (*u*NADW) compared to the lower NADW (*l*NADW) (Steinfeldt et al., 2009).

With respect to the inventory estimates from GLODAP-ΔC* the results are similar to the TTD ones north of 30ºS, mind the large amount of negative C_{ANT} estimates in the ΔC* approach caused by the high zero-C_{ANT} reference considered (Gruber et al., 1996; Matsumoto and Gruber, 2005). South of 30ºS the ΔC* method also shows low specific inventories of C_{ANT} (Fig. 4). Regarding these results, Lo Monaco et al. (2005) had already pointed out that the ΔC* yielded close to zero or even negative C_{ANT} values in AABW, while the rest of methods predicted concentrations ~10 μmol kg^{-1}. Compared with the specific inventories of C_{ANT} in the WOCE A14 (Vázquez-Rodríguez et al., 2009b), the results here obtained are very alike: in the equatorial and subtropical regions of the western Atlantic basin the ΔC* and TTD methods predict very similar inventory values and trends, but this similarity ceases south from 40ºS, where the influence of Antarctic origin waters starts to be sizeable. The here-accounted alkalinity offset and the corresponding increase in C_{ANT} specific inventory (~12 mol C m^{-2}) brings closer together the ΔC* inventory and all others (differences reduce by 35%, especially south of 40ºS) in Fig. 4. However, there are non-negligible remnant discrepancies, especially south of 35ºS, with the inventories from TTD, φC_T^o and TrOCA.

Lee et al. (2003) provided C_{ANT} inventories applying a slightly modified version of the ΔC* method and computed C_{ANT} specific inventories by latitude bands separately for the eastern and western Atlantic basins. The western Atlantic C_{ANT} inventories from Lee et al. (2003) (included in Fig. 4) are based on several cruises, including the WOCE A17. The basin wide inventories there described follow the same latitudinal trends as the WOCE A17 ones, except for the lower values south of 30ºS when compared to the φC_T^o, TTD and TrOCA estimates. Part of these lower values south of 30ºS (where only the section A17 was used to calculate inventories in

Lee's work) can also be justified from the unaccounted -8 μmol kg^{-1} offset in A_T data previously mentioned. On this regard, Ríos et al. (2003) had also described for the eastern Atlantic basin an increasing trend of C_{ANT} inventories southwards from the Equator up to the Southern Ocean. They used a carbon-based back-calculation method for their C_{ANT} estimates that yielded results in agreement with model outputs (Sarmiento et al., 1995). In addition to this reference, a set of different Ocean Global Circulation Models (Princeton/GFDL, MPI and Hadley OGCMs) have reproduced C_{ANT} specific inventories showing similar trends of southward increment, i.e., an increase of 20-25 mol C m^{-2} from latitude 10ºS to 50ºS (Orr et al., 2001). The above evidences support the C_{ANT} specific inventory results here obtained by the φC_T^o, TTD and TrOCA methods, especially south of 30ºS. This suggests revising the Atlantic and global C_{ANT} inventories based on much larger, updated and high-quality data collections with different calculation methods.

On average, the western Atlantic basin shows C_{ANT} specific inventories that are ~35% larger than those in the eastern basin between the Equator and 45ºS, compared with the work from Vázquez-Rodríguez et al. (2009b). This is congruent with the fact that the deep waters of the West Atlantic basin, i.e., NADW and AABW, are more ventilated and therefore have higher C_{ANT} burdens than those in the East Atlantic basin. As mentioned in the introductory section, the WOCE A17 tracks adequately the deep-water-bearing DWBC and facilitates making this inter-basin comparison.

5. Conclusions

This work examines the C_{ANT} distribution and inventories in the South Atlantic western basin calculated with data from the WOCE A17 cruise. The C_{ANT} estimates obtained with the ΔC^*, φC_T^o, TrOCA (all three corrected for the A_T offset reported in Ríos et al, 2005) and TTD methods show different concentration distributions depending on the water masses and

circulation. All methods reported the maximum values of C_{ANT} (50-60 μmol kg^{-1}) in the upper warm waters from the tropical gyres, where the SACW predominates. The TrOCA method gives the highest [C_{ANT}] values. In the upper layers, concentrations reach even over the theoretical limit of the C_{ANT} saturation for 1994. The minimum C_{ANT} values (~5 μmol kg^{-1}) from all methods are found in the oldest waters flowing northwards, at about 1000 dbar (*u*CDW) and around 3500 dbar (*l*CDW). The TTD and φC_T^o methods show similar distributions of these minimum values. The TrOCA and GLODAP-ΔC* methods both show the minima associated to the *u*CDW, but the minimum associated to the *l*CDW reaches the bottom in the case of TrOCA (unlike the TTD and φC_T^o methods) and it disappears in the case of the ΔC*. North of 15ºS the relative maxima are associated to the slightly more ventilated and younger *u*NADW and *l*NADW. The TrOCA approach gives the highest relative maximum in the *u*NADW of all four methods, being three times higher than the TTD method and two times higher than ΔC* and φC_T^o methods. The main overall discrepancies between the four methods correspond to the relative C_{ANT} maximum of the *l*NADW: this structure is well identified in the φC_T^o and TTD methods but seems to disappear in the case of TrOCA and GLODAP-ΔC*. South of 40ºS there is a slight increase of C_{ANT} below 4000 dbar originated by the penetration northwards of the AABW that is detected by the φC_T^o, TrOCA and TTD methods. The ΔC* approach consistently yielded negative estimates of C_{ANT} below ~2800 db (Fig. 3) that were not considered when computing column inventories of C_{ANT}.

In terms of specific inventories of the western Atlantic basin, the φC_T^o, TrOCA and TTD C_{ANT} estimation methods confirm an increasing tendency south from the Equator. Contrarily, the ΔC* method shows a decreasing trend south from 35ºS. South of 40ºS the average C_{ANT} inventory obtained from φC_T^o, TrOCA and TTD methods is significantly higher (~45%) than those in the GLODAP database calculated from the ΔC* method.

ACKNOWLEDGEMENTS

We would like to thank the captain, officers and crew of the R/V *Maurice Ewing* and all the participants of the CITHER–2 cruise. We are also very grateful to G. Rosón for his pH and alkalinity measurements. Special thanks go to M. Arhan (coordinator of the WOCE–France program CITHER) and L. Mémery (chief scientist of cruise CITHER-2). This work was developed and funded by the European Commission within the 6th Framework Programme (EU FP6 CARBOOCAN Integrated Project, Contract no. 511176) and by the Xunta de Galicia within the INCITE framework (M4AO project PGIDIT07PXB402153PR). Marcos Vázquez-Rodríguez was funded by the Consejo Superior de Investigaciones Científicas (CSIC) I3P predoctoral grant program REF.: I3P-BPD2005.

References

Alvarez-Salgado, X.A., Fraga, F., Pérez F.F., 1992. Determination of nutrient salts both in sea and brackish waters by automatic methods. The phosphate blank. Marine Chemistry 39, 311–319.

Anderson, L.A., Sarmiento J.L, 1994. Redfield ratios of remineralization determined by nutrient data analysis, Global Biogeochemical Cycles 8, 65–80.

Arhan, M. , Mercier, H., Bourlès, B., Gouriou, Y., 1998. Hydrographic sections across the Atlantic at 7º30N and 4º30S. Deep–Sea Res. Part I 45, 829–872.

Böning, C.W., Dispert, A., Visbeck, M., Rintoul, S.R., Schwarzkopf, F.U., 2008. The response of the Antarctic Circumpolar Current to recent climate change. Nature Geoscience 1, 864–869.

Brewer, P., 1978. Direct observation of the oceanic CO_2 increase. Geophysical Research. Letters 5, 997–1000.

Broecker, W.S., Peng, T.–H., 1982, Tracers in the Sea. Columbia University. Eldigio Press. New York, 690 pp.

Canadell, J., Le Quéré, C., Raupach, M. R. , Fields C., et al., 2007. Contributions to accelerating atmospheric CO_2 growth from economic activity, carbon intensity, and efficiency of natural sinks. Proceedings of National Academy Sciences 104(47), 18866–18870, doi:10.1073/ pnas.0702737104. vol. 104 no. 47

Chen, C.T., Millero, F.J., 1979. Gradual increase of oceanic carbon dioxide. Nature 277, 205–206.

Chung, S.-N., Lee, K., Feely, R. A., Sabine, C. L., Millero, F. J., Wanninkhof, R., Bullister, J. L., Key, R. M., and Peng, T.-H., 2003, Calcium carbonate budget in the Atlantic Ocean based on water column inorganic carbon chemistry, Global Biogeochem. Cycles, 17(4), 1093, doi:10.1029/2002GB002001.

Dengler, M., Schott, F.A., Eden, C., Brandt, P., Fischer, J., Zantopp, R.J., 2004. Break-up of the Atlantic deep western boundary current into eddies at 8ºS. Nature 432, 1018–1020.

Dickson, A.G., Millero, F.J., 1987. A comparison of the equilibrium constants for the dissociation of carbonic acid in seawater media, Deep Sea Research I 34, 1733–1743.

Groupe CITHER-2, Le, 1995. Recueil de données, campagne CITHER-2, R/V Maurice Ewing (4 janvier–21 mars 1994). Volume 2: CTD-O2. Rapport Interne LPO 95-04, 520 pp.

Groupe CITHER-2, Le, 1996. Recueil de données, campagne CITHER-2, R/V Maurice Ewing (4 janvier–21 mars 1994). Volume 1: Mesure 'en route', parameters méthéorologiques, bathymetrie et courantométrie Doppler. Rapport Interne LPO 96-01, 180p.

Gruber, N., Sarmiento, J.L, Stocker. T.F., 1996. An improved method for detecting anthropogenic CO_2 in the oceans. Global Biogeochemical Cycles 10, 809–837.

Johnson, K.M., Wills, K.D., Butler, D.B., Johnson, W.K., Wong C.S., 1993. Coulometric total carbon dioxide analysis for marine studies: maximizing the performance of an automated gas extraction system and coulometric detector. Marine Chemistry 17, 1–21.

Key, R.M., Kozyr, A. , Sabine, C.L., Lee, K., Wanninkhof, R., et a., 2004. A global ocean carbon climatology: Results from Global Data Analysis Project (GLODAP). Global Biogeochemical Cycles 18, GB4031, doi:10.1029/2004GB002247.

Körtzinger, A., Mintrop, L., Duinker, J.C., 1998. On the penetration of anthropogenic CO_2 into the North Atlantic ocean. Journal of Geophysical Research 103, 18681–18689.

LeQuéré C., Rödenbeck, C., Buitenhuis, E.T., Conway, T.J., et al., 2008. Saturation of the Southern Ocean CO_2 Sink Due to Recent Climate Change. Science 316, 1735-1738.

Lee, K., Choi, S.-D. Park, G.-H. Wanninkhof, R., et al.. 2003. An updated anthropogenic CO_2 inventory in the Atlantic Ocean. Global Biogeochemical Cycles 17 (4), 1116, doi: 10.1029/2003GB002067.

Lo Monaco, C., Goyet, C., Metzl, N., Poisson, A., Touratier, F., 2005. Distribution and inventory of anthropogenic CO_2 in the Southern Ocean: Comparison of three data-based methods. *J. Geophys. Res*. 110, C09S02, doi:10.1029/2004JC002571.

Manabe, S., Stouffer. R., 1993. Century-scale effects of increased atmospheric CO_2 on the ocean–atmosphere system, Nature 364, 215–218

Matear, R.J., Wong, C.S., Xie, L., 2003. Can CFCs be used to determine anthropogenic CO_2? Global Biogeochem. Cycles 17, doi:10.1029/2001GB001415.

Matsumoto, K., Gruber. N., 2005. How accurate is the estimation of anthropogenic carbon in the ocean? An evaluation of the ΔC* method. Global Biogeochemical Cycles 19, doi: 10.1029/2004GB002397.

Mehrbach, C., Culberson, C.H., Hawley, J.E., Pytkowicz, R.M., 1973, Measurements of the apparent dissociation constant of carbonic acid in seawater at atmospheric pressure. Limnology and Oceanography 8, 897–907.

Mémery, L., Arhan, M., Álvarez-Salgado, X.A., Messias, M.-J., et al., 2000. The water masses along the western boundary of the south and equatorial Atlantic, Progress in Oceanography 47, 69–98.

Mercier, H.,M. Arhan, 1997. Two meridional hydrographic sections in the eastern South Atlantic Ocean (WHP lines A13 and A14), Intl. WOCE Newsl. 28, 28–30.

Mintrop, L., Pérez, F.F., Gonzalez-Dávila, M., Santana-Casiano, M.J., Kortzinger, A., 2002. Alkalinity determination by potentiometry: Intercalibration using three different methods. Ciencias Marinas 26(1), 23–37.

Mouriño, C., Fraga, F., 1985. Determinacion de nitratos en agua de mar. Investigacion Pesquera 49, 81–96.

Orr, J.E., Maier-Reimer, E., Mikolajewicz, U., Monfray, P., et al., 2001. Estimates of anthropogenic carbon uptake from four three-dimensional global ocean models, Global Biogeochemical Cycles 15 (1), 43–60.

Pérez, F.F., Álvarez, M., Ríos, A.F., 2002, Improvements on the back-calculation technique for estimating anthropogenic CO_2. Deep-Sea Res. I 49, 859–875.

Pérez, F.F., Fraga, F., 1987a. The pH measurements in seawater on NBS scale. Marine Chemistry 21, 315–327.

Pérez, F.F., Fraga, F., 1987b. A precise and rapid analytical procedure for alkalinity determination. Marine Chemistry 21, 169–182.

Redfield, A. C., Ketchum,, B. H., Richards, F. A.,1963. The influence of organisms on the composition of sea-water. The Sea 2, 26–77.

Ríos, A.F., Alvarez-Salgado, X.A., Pérez, F.F., Bingler L.S., Arístegui, J. Mémery, L., 2003. Carbon dioxide along WOCE line A14: Water masses characterization and anthropogenic entry. Journal Geophysical Research 108(C4), 3123, doi:10.1029/2000JC000366.

Ríos, A.F., Anderson, T.R., Pérez, F.F., 1995, The carbonic system distribution and fluxes in the NE Atlantic during Spring 1991, Prog. Oceanog. 35, 295–314.

Ríos, A.F., Johnson, K.M., Álvarez-Salgado, X.A., et al., 2005. Carbon dioxide, hydrographic, and chemical data obtained during The R/V Maurice Ewing Cruise in the South Atlantic Ocean (WOCE Section A17, 4 January - 21 March 1994), Carbon Dioxide Information Analysis Center, Oak Ridge National Laboratory, ORNL/CDIAC- 148, NDP-084, 1-27.

Robertson, J.E., Robinson, C., Turner, D.R., Holligan, P., et al., 1994. The impact of a coccolithophore bloom on oceanic carbon uptake in the northeast Atlantic during summer 1991. Deep–Sea Research I 41, 297–314.

Sabine C.L., Feely, R.A., Gruber, N., Key, R.M. et al., 2004. The oceanic sink for anthropogenic CO_2. Science 305, 367–371.

Sarmiento, J.L., Le Quéré, C., 1996. Oceanic carbon dioxide uptake in a model of century-scale global warming, Science 274, 1346–1350,

Sarmiento, J.L., Murnane, R., Le Quere C., 1995. Air-sea CO_2 transfer and the carbon budget of the North Atlantic, Phil. Trans. R. Soc. London 348, 211–219.

Sarmiento, J.L., Hughes, T.M.C., Stouffer, R.J., Manabe, S., 1998. Simulated response of the ocean carbon cycle to anthropogenic climate warming, Nature 393, 245–249,

Steinfeldt, R., Rhein, M., Walter, M., 2007. NADW transformation at the western boundary between 66ºW-20ºN and 60ºW-10ºN. Deep-Sea Research I 54, 835–855.

Steinfeldt, R., Rhein, M., Bullister, J.L., Tanhua T., 2009. Inventory changes in anthropogenic carbon from 1997–2003 in the Atlantic Ocean between 20°S and 65°N, Global Biogeochemical Cycles 23, doi:10.1029/2008GB003311.

Touratier, F., Azouzi, L., Goyet, C., 2007. CFC-11, Δ14C and 3H tracers as a means to assess anthropogenic CO_2 concentrations in the ocean. Tellus 59B, 318–325, doi: 10.1111/j.1600-0889.2006.00247.x.

Vázquez-Rodríguez, M., Padin, X.A., Ríos, A.F., Bellerby, R.G.J., Pérez, F.F., 2009a. An upgraded carbon-based method to estimate the anthropogenic fraction of dissolved CO_2 in the Atlantic Ocean. Biogeosciences Discuss. 6, 4527–4571.

Vázquez-Rodríguez, M., Touratier, F., Lo Monaco, C., Waugh, D.W., Padin, X.A., et al., 2009b. Anthropogenic carbon distributions in the Atlantic Ocean: Databased estimates from the Arctic to the Antarctic, Biogeosciences 6, 439–451.

Waugh, D.W., Hall, T.M., McNeil, B.I., Key, R., Matear, R.J., 2006. Anthropogenic CO_2 in the oceans estimated using transit time distributions, Tellus, 58B, 376-389, DOI: 10.1111/j.1600-0889.2006.00222.x.

Weiss, R.F., Bullister, J.L., Gammon, R.H. Warner, M.J., 1985. Atmospheric chlorofluoromethanes in the deep equatorial Atlantic. Nature 314, 608–610.

Yool, A., Oschlies, A., Nurser, A.J.G., Gruber, N., 2010. A model-based assessment of the TrOCA approach for estimating anthropogenic carbon in the ocean, Biogeosciences 7, 723–751.

Figure captions

Figure 1 Map of the eastern South Atlantic Ocean showing the position of the 107 full–depth stations surveyed during the CITHER-2 (WOCE A17) cruise.

Figure 2 Vertical profiles of measured θ (ºC), salinity, [$Si(OH)_4$] (μmol kg^{-1}), calculated Apparent Oxygen Utilisation (AOU; μmol kg^{-1}), $CaCO_3$ dissolution (ΔCa; μmol kg^{-1}) and water mass age (years) from CFC12 data. The acronyms of the main water masses present along the WOCE A17 line are labeled on the θ (SACW, *u*NADW, *l*NADW, *u*CDW, *l*CDW and AABW) and salinity (AAIW) plots.

Figure 3 Vertical profiles of C_{ANT} along the WOCE A17 line according to four different estimation approaches: the φC_T^o, the GLODAP-ΔC*, the TrOCA and the TTD methods. All concentrations are in μmol kg^{-1}. The reported -8 μmol kg^{-1} A_T offset (Ríos et al., 2005) has been considered and corrected for in all three C_{ANT} back-calculation approaches, i.e., φC_T^o, GLODAP-ΔC* and TrOCA. The spots where negative C_{ANT} estimates were predicted by the ΔC* method have been automatically set to zero and filled with a light purple color. They are located below the C_{ANT}=0 isopleth (pressures > ~2800 dbar).

Figure 4 C_{ANT} specific inventories were estimated by vertical integration. The uncertainties of these estimates were calculated by means of random propagation with depth of an average 5.2 μmol kg^{-1} standard error of the C_{ANT} estimate over 100 perturbation iterations. Assuming that the uncertainties attached to the C_{ANT} estimation method are purely random and do not introduce biases, the final error is calculated by propagating the individual errors associated to the samples. They reflect both measurement and parameterization errors. For each of the considered latitude belts the mean of the integrated values at each station was calculated. The error bars here shown were computed as the confidence intervals of the mean.

Figure 1

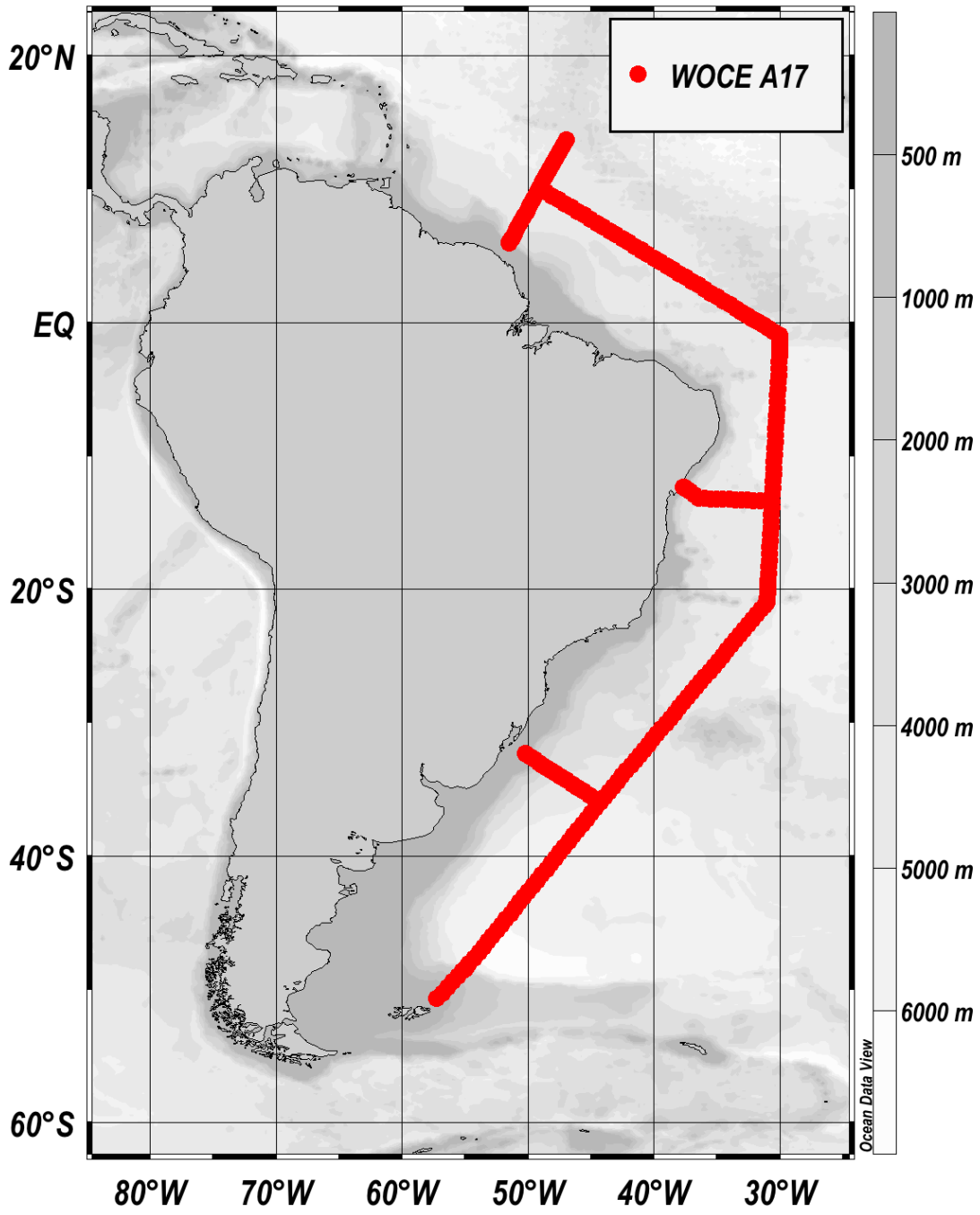
WOCE A17
20°N
EQ
20°S
40°S
60°S
80°W
70°W
60°W
50°W
40°W
30°W
500 m
1000 m
2000 m
3000 m
4000 m
5000 m
6000 m
Ocean Data View

Figure 2

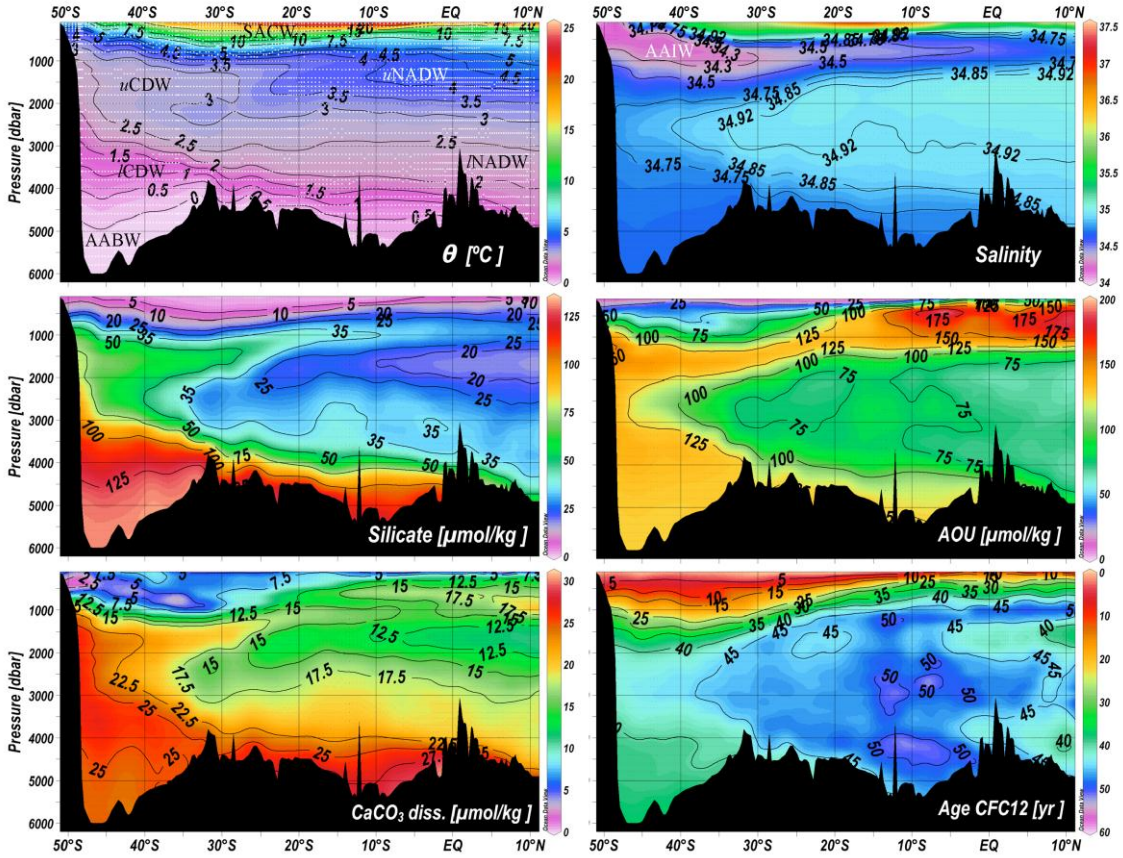
50°S
40°S
30°S
20°S
10°S
EQ
10°N
Pressure [dbar]
SACW
uCDW
lCDW
uNADW
lNADW
AABW
θ [°C]
AAIW
Salinity
Silicate [µmol/kg]
AOU [µmol/kg]
CaCO3 diss. [µmol/kg]
Age CFC12 [yr]

Figure 3

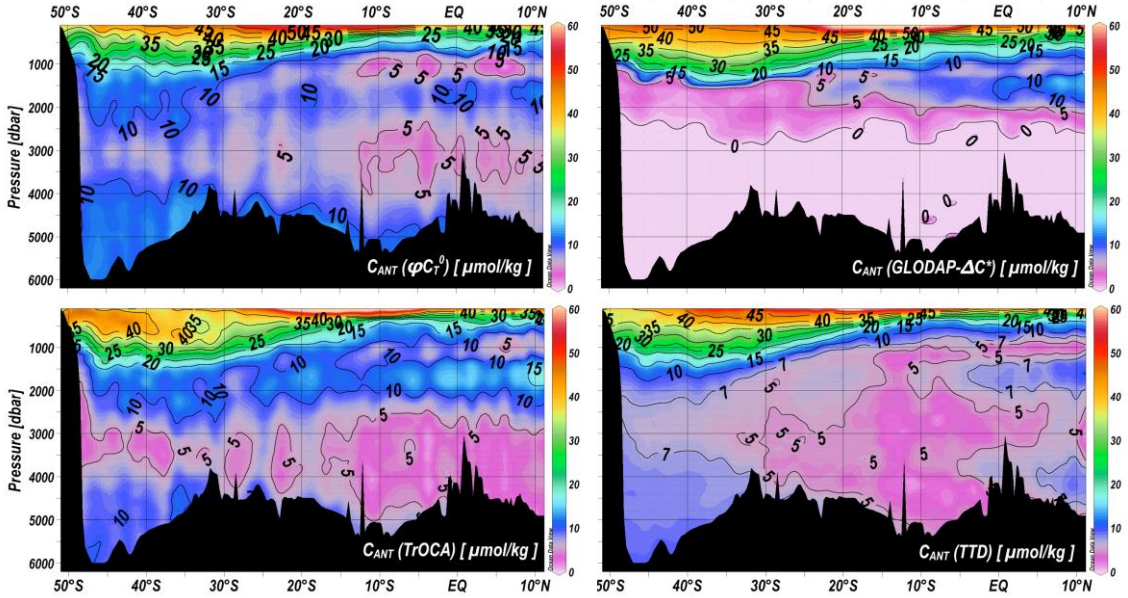
50°S
40°S
30°S
20°S
10°S
EQ
10°N
Pressure [dbar]
1000
2000
3000
4000
5000
6000
C_{ANT} (φC_T^0) [µmol/kg]
C_{ANT} (GLODAP-ΔC*) [µmol/kg]
C_{ANT} (TrOCA) [µmol/kg]
C_{ANT} (TTD) [µmol/kg]
Ocean Data View

Figure 4

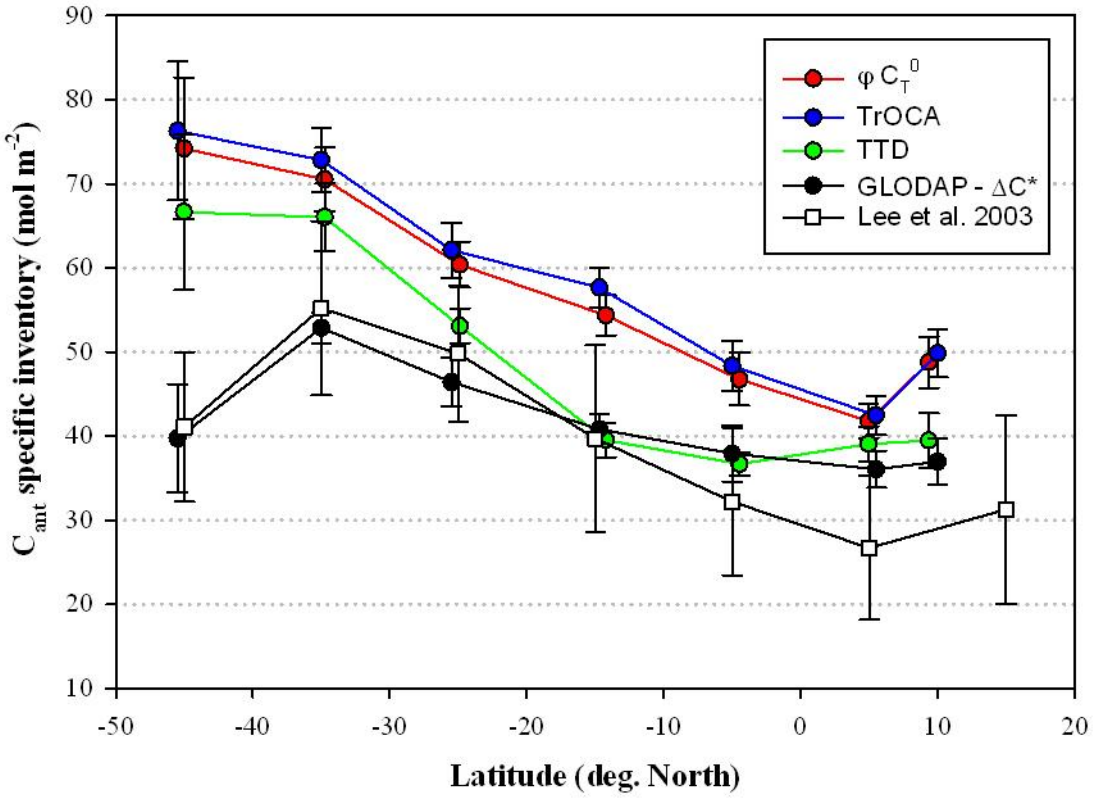
90
80
70
60
50
40
30
20
10
-50
-40
-30
-20
-10
0
10
20
C_ant specific inventory (mol m^-2)
Latitude (deg. North)
φ C_T^0
TrOCA
TTD
GLODAP - ΔC*
Lee et al. 2003